SECED - Society for Earthquake and Civil Engineering Dynamics
Young Engineers Conference - 2013

STRUCTURAL HEALTH MONITORING OF CIVIL INFRASTRUCTURE USING WIRELESS SENSOR NETWORKS

N. de Battista[1*], J. A. Rice[2], S.-H. Sim[3], J. M. W. Brownjohn[4] and H. P. Tan[5]

[1] *PhD student, Dept. of Civil and Structural Engineering, The University of Sheffield, Sheffield UK.*
[2] *Assistant Professor, Eng. School of Sustainable Infrastructure & Environment, University of Florida, FL, USA.*
[3] *Assistant Professor, Ulsan National Institute of Science and Technology, Ulsan, Republic of Korea.*
[4] *Professor, College of Engineering, Mathematics and Physical Sciences, University of Exeter, Exeter, U.K.*
[5] *Senior Scientist, Institute for Infocomm Research (I2R), A*STAR, Singapore*
** Email: nickydebattista@gmail.com*

ABSTRACT

Eight wireless accelerometer sensor nodes (Imote2), each equipped with an energy harvesting solar panel, were deployed continuously on an operational pedestrian footbridge in Singapore for two weeks. The sensor nodes periodically acquired and processed vibration data using a novel embedded data processing algorithm, referred to as the Filtered Hilbert-Huang transform, resulting in a 96% data reduction. From the processed results which the nodes transmitted to the base station, it was possible to conclude that resonant response from pedestrian walking excitation was the cause of increased vibration levels during peak usage times. The maximum recorded peak and RMS vibration were 52mg and 35mg respectively, which are within the limits allowed by several major design guidelines. This wireless sensor network deployment demonstrated the potential of decentralised, embedded data processing for wireless medium- to long-term structural health monitoring of civil infrastructure.

1. INTRODUCTION

Wireless sensor networks (WSNs) are becoming an efficient and cost-effective solution to structural health monitoring (SHM) applications where the use of data cables is prohibitively expensive or impossible. Besides removing the need for labour-intensive data cable installation, WSNs offer the possibility of carrying out distributed, decentralised data processing. Rather than transmitting all the raw data back to a central repository for post-processing (as is done with wired sensor networks), the microcontroller that is part of every WSN node can be used to process the raw data and transmit to the base station only the required results. When used carefully, this has the advantage of reducing the amount of data that needs to be transmitted, with associated benefits in wireless communication reliability, power saving and data management.

The technique of decentralised, embedded data processing (EDP) has been demonstrated in the past, using various algorithms to carry out model identification (Sim et al., 2010; Dorvash & Pakzad, 2012) and to estimate structural parameters such as natural frequencies (Feltrin et al., 2010; Y Lei et al., 2010) and cable tension (Cho et al., 2010). In general, WSN nodes periodically acquire data which are either processed individually on each node or within clusters of nodes. The individual nodes or cluster heads would then transmit the estimated results to the base station (also referred to as the gateway node or data sink) and discard the raw data.

This study presents the use of a novel algorithm, referred to as the Filtered Hilbert-Huang transform (FHHT), for carrying out EDP on WSNs. It is based on the Hilbert-Huang transform (Huang & S. S. P. Shen, 2005) with modal separation using a bandpass filtering approach (Yang et al., 2003), combined with the Random Decrement technique (Asmussen et al., 1998). Deployed over a period of time, this FHHT-based EDP technique can be used to track temporal variations in a structure's dynamic behaviour.

Following a brief overview of the FHHT algorithm, this paper describes a two-week WSN monitoring deployment on a footbridge in Singapore. Each sensor node periodically acquired vibration data, processed them using the embedded FHHT algorithm and transmitted the results to the gateway node. This automated monitoring provided some interesting information about the use and performance of the footbridge. The conclusions of the investigation helped to determine the cause of disturbing vibrations which had been reported by pedestrians using the bridge.

2. FILTERED HILBERT-HUANG TRANSFORM FOR EMBEDDED DATA PROCESSING IN WIRELESS SENSOR NETWORKS

The FHHT-based EDP method comprises the following steps:
Step 1 - Digital high-pass filtering of data to eliminate low-frequency noise. In this deployment, a 6th order Butterworth filter with a cutoff frequency of 1Hz was used.
Step 2 - Calculation of two signal properties at fixed intervals of the data. The user can choose from: peak acceleration; peak to peak acceleration; root mean squared (RMS) acceleration; peak dynamic displacement; peak to peak dynamic displacement; and frequency-weighted R factor for vibration serviceability assessment (British Standards Institution, 1987).
Step 3 - Mode separation by digital bandpass filtering (one filter per mode of interest). After inspecting the frequency content of a sample signal collected before monitoring, each filter's pass-bands can be set to retain a single vibration mode of interest, while allowing for any possible shift in natural frequency over time.
Step 4 - The Empirical Mode Decomposition (Huang et al., 1998) is applied to each filtered mode signal. This makes each mode signal a 'monocomponent', which is effectively an estimate of the mode's contribution to the whole signal. The modal RMS acceleration is obtained from the RMS of the monocomponent.
Step 5 - The Random Decrement technique (Asmussen et al., 1998) is used to estimate the free decay of each monocomponent in segments. The modal damping ratio of each segment is estimated from the logarithmic decrement of the segment's free decay.
Step 6 - The Hilbert transform (Bendat & Piersol, 2010) is applied to each monocomponent to obtain its complex analytic signal. From the analytic signals, the quasi-instantaneous natural frequencies (Huang et al., 2009) of the vibration modes of interest are estimated at regular intervals.
Step 4 followed by step 6 are commonly known as the Hilbert-Huang transform. In combination with the rest of the FHHT steps described above, the raw vibration data can be reduced to a few parameters pertaining to the overall signal (step 1) and to any number of its individual modes of vibration (amplitude in step 4, damping ratio in step 5 and natural frequency in step 6), estimated at regular, closely-spaced intervals.
The FHHT algorithm was developed in such a way that it is implementable on low-power microcontrollers found on WSN platforms. A research collaboration was initiated between the authors in order to write the software in the C and nesC programming languages as an add-on to the open-source ISHMP Toolsuite (Rice et al., 2010) and embed and test it on the Imote2 WSN platform.

3. WIRELESS STRUCTURAL HEALTH MONITORING USING EMBEDDED DATA PROCESSING

Following a series of verification lab tests, the FHHT method embedded on the Imote2 WSN platform was used to monitor the Labrador Park pedestrian overhead bridge (POB) in Singapore, for two weeks from 11th to 25th April 2013.

Labrador Park Pedestrian Overhead Bridge

The POB (Figure 1) is a seven-span footbridge located in the south of Singapore, linking the Labrador Park Mass Rapid Transit (MRT) station to the PSA building, which houses commercial outlets and offices. The four

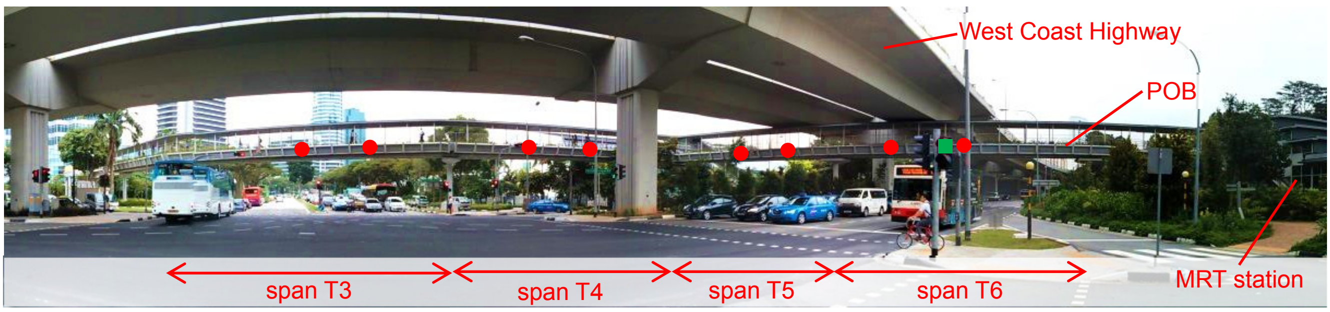

Figure 1. The Labrador Park pedestrian overhead bridge (POB) in Singapore. The red circles and green square indicate the approximate locations of the 8 remote and 1 gateway nodes respectively.

longer spans, referred to as T3 (33.66m span), T4 (31.61m span), T5 (26.17m span) and T6 (28.44m span), cross the northbound and southbound lanes of Alexandra Road and the eastbound and westbound lanes of Telok Blangah Road, respectively. T5 and T6 pass under the West Coast Highway, which runs parallel to Telok Blangah Road.

Each span comprises a simply-supported, structural steel, square hollow section truss. The bridge deck consists of a composite concrete slab cast on permanent steel formwork which is anchored to the trusses' top chords. The deck is shaded by a steel purlin and decking roof supported by steel circular hollow section columns.

The Land Transport Authority (LTA, Singapore) received a number of public complaints about disturbing vibrations being felt by pedestrians using the POB, particularly on spans T3 and T6. An independent study which was carried out in May 2012 on these two spans, using wired accelerometers and strain gauges, concluded that the main cause of vibration was due to pedestrian traffic. It also found that the first vertical natural frequency of T3 was excitable in resonance by the first harmonic of pedestrian walking forces (Middleton & Brownjohn, 2012).

The aim of the present study was to monitor all of the four main spans (T3 to T6) over a period of time, in order to obtain further information about their daily vibration pattern and how it related to the dynamic properties of the bridge.

Wireless Sensor Network Deployment

The WSN deployed on the Labrador Park POB consisted of eight data collection remote nodes and one gateway node. The remote nodes were placed on the outer edge of the trusses (out of reach), at approximately the mid-span and quarter-span points of the T3, T4, T5 and T6 spans of the POB (Figure 1). The gateway node was placed close to the mid-span of T6 (shaded by the expressway above the POB).

Each remote node (Figure 2a) consisted of an IPR2400 Imote2 wireless platform, an ISM400 accelerometer sensor board (formerly known as SHM-A), an IBB2400 battery board and a *Tenergy* 15.6Ah Li-Ion battery, which was recharged via an *Adafruit Industries* USB/DC/Solar Lithium Ion/Polymer charger (v.1.0). All the components were secured in an ABS weatherproof enclosure which was mounted on the steel truss using a strong magnet. A *Voltaic Systems* 3.4W 6V solar panel was wired to the charging circuit in each node. Four of the remote nodes which were constantly exposed to direct sunlight were protected with an insulating polystyrene box with a reflective foil outer layer (Figure 2b) to prevent them from overheating.

The gateway node (Figure 2c) consisted of an IPR2400 Imote2, an IBB2400 battery board and an IIB2400 interface board, connected with a USB cable to a *Samsung* NC110 netbook. A *Huawei* 3G / Wi-Fi modem was used to provide the netbook with internet access, both for remote control (using *TeamViewer*) and for automatic data transfer (using *Dropbox*). All the components were enclosed in a metal weatherproof enclosure provided by *Tritech Ltd*. A USB webcam attached to the underside of the footbridge roof captured images of the deck at 30s intervals. In order to increase the wireless signal strength, a *TP-Link* TL-ANT2408CL 2.4GHz 8dBi high-gain, omni-directional antenna was mounted on a magnetic base and connected to each node (remote and gateway) with a 1.5m coaxial cable.

FHHT monitoring events were programmed to occur every 30 minutes. Each event started with the remote nodes being woken up from their sleep state to have their battery levels checked and their clocks synchronised by the gateway node. The remote nodes then acquired 10 minutes of vibration data in the vertical direction at a

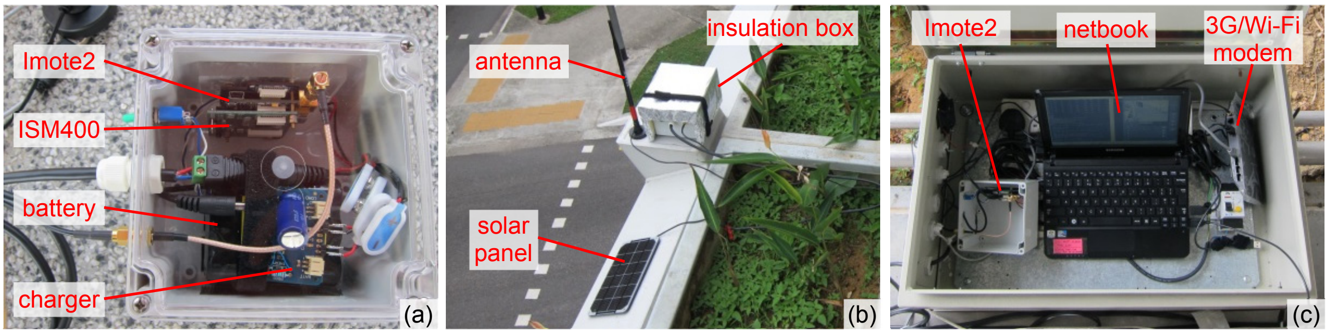

Figure 2. (a) An assembled remote node in a weatherproof enclosure; (b) a complete remote node installed on the footbridge; (c) the gateway node installed on the footbridge.

sampling rate of 100Hz and processed them with the FHHT filters and processing parameters sent by the gateway node. The results were then transmitted from each of the remote nodes, in turn, to the gateway node which stored them in a text file on the netbook. The remote nodes then went back into a low-power sleep state, waking up every 10s for 500ms to listen for transmissions from the gateway node.

Thus, ten minute snapshots of the bridge performance were obtained every half an hour. These consisted of:

- peak and RMS acceleration at 1s intervals, at mid- and quarter-spans (11th to 18th April);
- peak to peak dynamic displacement and R-factor at 1s intervals, at mid- and quarter-spans (18th to 25th April);
- maximum RMS acceleration and natural frequency of the first (mid-span) and second (quarter-span) vertical modes of vibration, at 1s intervals; and
- damping ratio of the first (mid-span) and second (quarter-span) vertical modes of vibration, at 20s intervals.

By processing the raw data with the embedded FHHT algorithm, the 60000 data points acquired by each remote node during a monitoring event were reduced to just 2430 values, representing a data reduction of 96%.

4. STRUCTURAL HEALTH MONITORING RESULTS AND DISCUSSION

The signal parameters recorded throughout the monitoring exercise are shown in Figure 3. As expected, the overall daily maximum amplitudes of all the recorded parameters are higher on weekdays than on weekends, since the Labrador Park POB is used mostly by commuters walking between the MRT station and the nearby office buildings. Figure 4 shows what the average weekday usage trend looks like. The highest amplitudes were

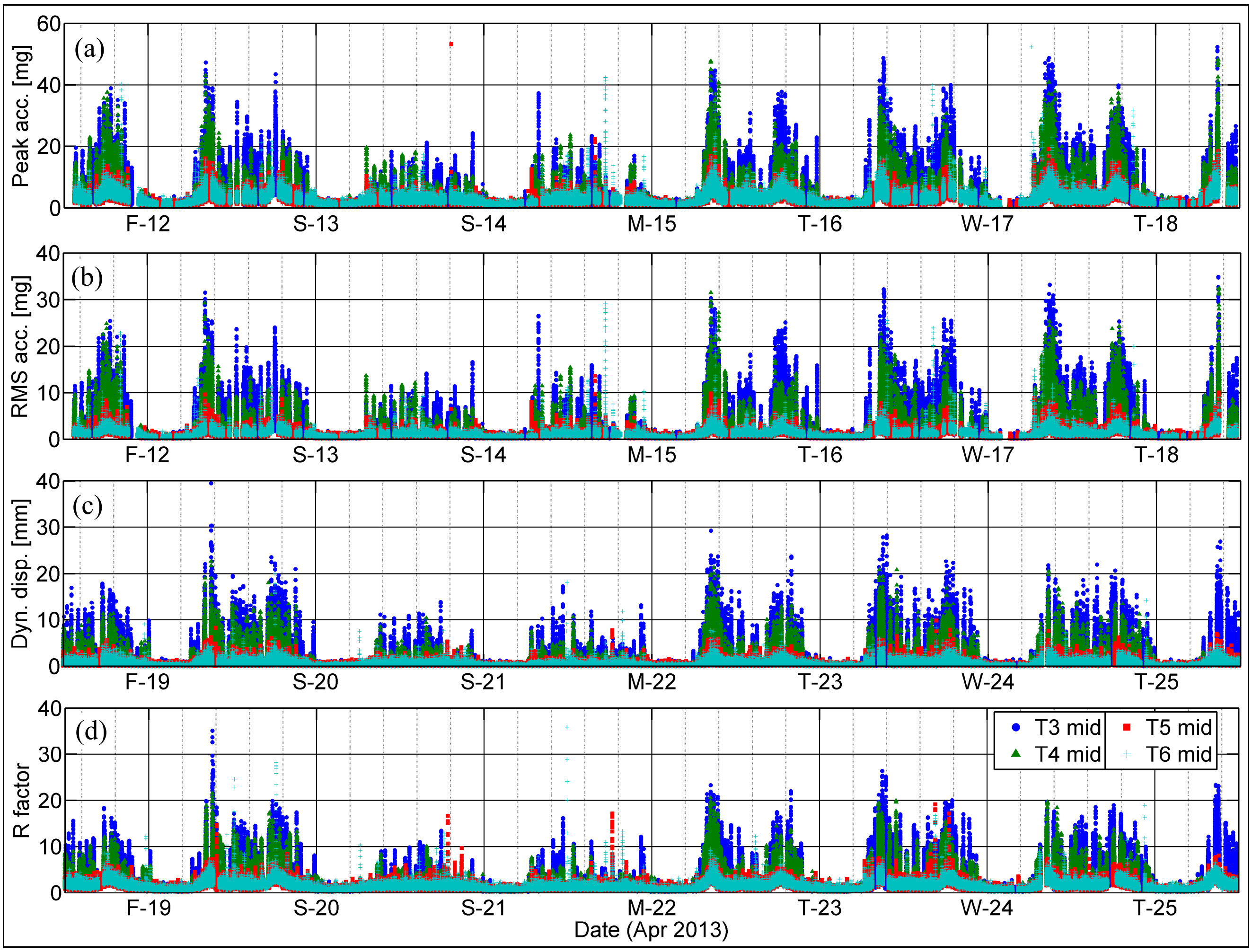

Figure 3. Signal parameters recorded during the two weeks of monitoring: a) peak acceleration, b) RMS acceleration, c) peak to peak dynamic displacement and d) R factors, calculated at 1s intervals from the mid-span acceleration data.

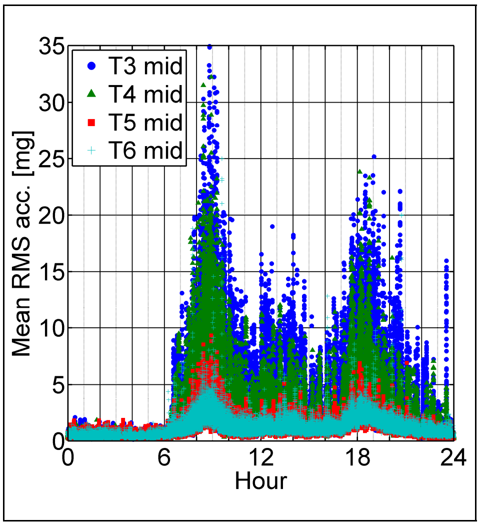

Figure 4. One-day mean of the RMS acceleration records acquired on weekdays from 11th to 18th April.

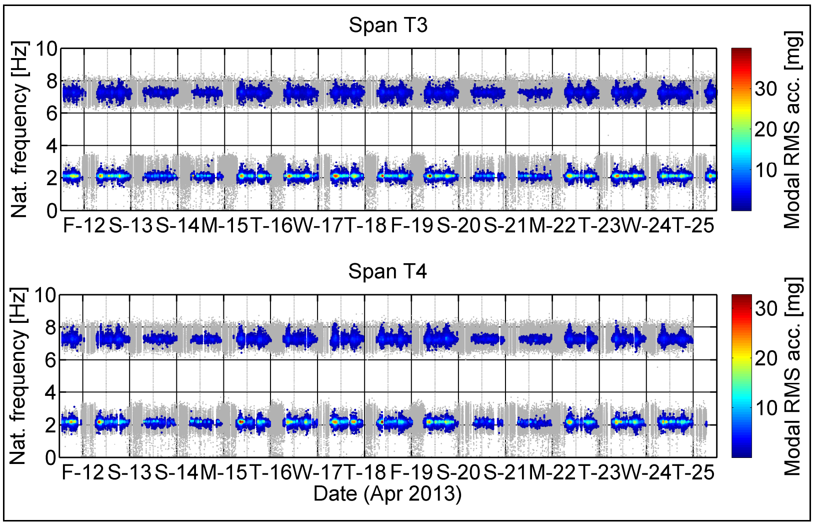

Figure 5. Natural frequencies of the first two vertical vibration modes of spans T3 and T4. Points in grey correspond to instances where the vibration energy was too low (modal RMS acceleration < 1mg) to enable a reliable frequency estimate.

recorded during the morning rush hour (~ 7:30am – 10:30am), followed by the evening rush hour (~ 5:30pm – 9:00pm). A lower increase in amplitude was also recorded during the lunch break hours (~ 12 noon – 3:00pm). During MRT non-service hours (~ 12 midnight – 5:30am), the vibration amplitude was much lower.

Table 1 shows the maximum values recorded from the four spans over the two-week monitoring period. The strongest sustained dynamic responses were recorded on span T3 (52mg peak), followed by T4 (48mg peak). Span T6 (52mg peak) also reached high levels of response but these were occasional and lasted for a short time.

According to the BD37/01 (The Highways Agency, 2001) guidance, the peak acceleration of T3 and T4 should not exceed 74mg. The British National Annex to Eurocode 1 (British Standards Institution, 2008) and the French Sétra footbridge design guidance (Sétra, 2006) both limit the acceptable peak acceleration of the POB to 102mg for a mean comfort level. Following the Concrete Society's TR43 Appendix G (Concrete Society, 1994), an upper limit of 128 on the R factor could be deemed reasonable for the POB. The vibration levels recorded on all four spans appear to be acceptable for human comfort, according to all of these documents.

The main reason behind the strong response to human traffic in spans T3 and T4 can be deduced from the time-frequency plots in Figure 5. The first vertical natural frequency of these two spans was found to be approximately 2.13Hz and did not appear to vary significantly over time. This falls within the range of normal walking pacing rates. Therefore the first vertical vibration mode of these two spans is susceptible to resonant excitation from human walking. As can be seen from the colour coding in **Error! Reference source not found.**, this mode dominated the overall response of spans T3 and T4.

The first vertical natural frequency of span T5 was also approximately 2.13Hz. However, since it is shorter than T3 and T4, the vibration levels attained on T5 were consistently lower. In the case of T6, the first vertical natural frequency was approximately 2.59Hz, which is slightly higher than the normal walking pacing rates. Therefore it is likely that T6 exhibits mostly off-resonant response, with sudden increases in amplitude corresponding to occasional fast walking speeds.

Table 1. Maximum signal parameters recorded at the mid-spans.

Span:	T3	T4	T5	T6
Peak acceleration [mg]	52	48	22 *	52
RMS acceleration [mg]	35	33	14	29
Dynamic displacement (peak to peak) [mm]	39	23	10	20
Frequency-weighted R factor	35	22	19	36

* Outlier value of 53mg recorded on 13th April at 19:20:35 is excluded.

5. CONCLUSION

A novel method for carrying out embedded data processing (EDP) in wireless sensor networks has been presented in this paper. This method, referred to as the Filtered Hilbert-Huang transform, was used to monitor the four longer spans of the Labrador Park pedestrian overhead bridge (POB) in Singapore for two weeks in April 2013. The FHHT results obtained from the wireless monitoring exercise showed that resonant vibration in the first vertical mode was responsible for the bulk of the response in the critical spans. Despite public complaints, the vibration levels of the POB were found to be within the limits specified in several major design guidelines. FHHT-based EDP, as demonstrated in this study, is expected to be a useful tool for medium- and long-term wireless monitoring of the vibration performance and tracking of dynamic properties of structures.

ACKNOWLEDGEMENTS

The authors are grateful to Ang Wee Boon, Tritech Group Ltd., Chua Hiang Ping, Rama Venkta, LTA and SMRT (Singapore) for assisting with the Labrador Park POB WSN deployment. This research was funded by EPSRC grant EP/G061130/1 (University of Sheffield) and by the “Sense and Sense-abilities” program (I^2R). The first author is supported by the University of Sheffield and A*STAR under the joint ARAP scholarship scheme.

REFERENCES

Asmussen, J.C., Ibrahim, S.R. and Brincker, R. (1998). Random decrement: Identification of structures subjected to ambient excitation. In *Proceedings of the 16th International Modal Analysis Conference (IMAC XVI)*. Santa Barbara, CA, USA: Society for Experimental Mechanics, pp. 914–921.
Bendat, J.S. and Piersol, A.G. (2010). The Hilbert transform. In *Random Data: Analysis and Measurement Procedures*. John Wiley and Sons, pp. 473–503.
British Standards Institution (1987). *BS 6841:1997. Guide to Measurement and evaluation of human exposure to whole-body mechanical vibration and repeated shock*, BSI, U.K.
British Standards Institution (2008). *UK National Annex to BS EN 1991-2:2003. Eurocode 1. Actions on structures. Traffic loads on bridges*, BSI, U.K.
Cho, S., Yun, C.-B. and Lynch, J.P. (2010). Smart wireless tension force monitoring system for stay cables. In *Proceedings of the 5th International Conference on Bridge Maintenance, Safety and Management (IABMAS)*. Philadelphia, PA, USA, pp. 152–159.
Concrete Society (1994). *Technical report no. 43. Post-tensioned concrete floors. Design handbook* 2nd ed. U.K
Dorvash, S. and Pakzad, S.N. (2012). Stochastic iterative modal identification algorithm and application in wireless sensor networks. *Structural Control and Health Monitoring*.
Feltrin, G. et al. (2010). Long-term monitoring of cable stays with a wireless sensor network. *Structure and Infrastructure Engineering*, 6:5,535–548.
Huang, N.E. et al. (2009). On instantaneous frequency. *Advances in Adaptive Data Analysis*, 1:2,177–229.
Huang, N.E. et al. (1998). The empirical mode decomposition and the Hilbert spectrum for nonlinear and non-stationary time series analysis. *Proceedings of the Royal Society A: Mathematical, Physical and Engineering Sciences*, 454:1971,903–995.
Huang, N.E. and Shen,S.S.P. (2005). *Hilbert-Huang transform and its applications*, World Scientific Publishing.
Lei, Y et al. (2010). Intelligent wireless sensors with application to the identification of structural modal parameters and steel cable forces: from the lab to the field. *Advances in Civil Engineering*, 2010:1–9.
Middleton, C.J. and Brownjohn, J.M.W. (2012). *Final report: POB bridge - Modal testing*. Unpublished.
Rice, J.A. et al. (2010). Flexible smart sensor framework for autonomous structural health monitoring. *Smart Structures and Systems*, 6:5-6,423–438.
Sétra (2006). *Footbridges. Assessment of vibrational behaviour of footbridges under pedestrian loading*, Sétra.
Sim, S.-H. et al. (2010). Automated decentralized modal analysis using smart sensors. *Structural Control and Health Monitoring*, 17:8,872–894.
The Highways Agency (2001). *BD37/01. Loads for highway bridges*, U.K.
Yang, J.N. et al. (2003). System identification of linear structures based on Hilbert-Huang spectral analysis. Part 1: normal modes. *Earthquake Engineering & Structural Dynamics*, 32:9,1443–1467.